the plant journal

SEB SOCIETY FOR EXPERIMENTAL BIOLOGY

The Plant Journal (2010) **61**, 191–199 doi: 10.1111/j.1365-313X.2009.04050.x

Tissue layer specific regulation of leaf length and width in Arabidopsis as revealed by the cell autonomous action of *ANGUSTIFOLIA*

Yang Bai[1,†], Stefanie Falk[1,†], Arp Schnittger[2,†], Marc J. Jakoby[1] and Martin Hülskamp[1,*]

[1]*Botanical Institute III, University of Köln, Gyrhofstrasse 15, 50931 Köln, Germany, and*

[2]*Institut de Biologie Moléculaire des Plantes du CNRS, IBMP-CNRS – UPR2357, 12 Rue du Général Zimmer, 67084 Strasbourg, France*

Received 29 July 2009; revised 11 September 2009; accepted 25 September 2009; published online 9 November 2009.
*For correspondence (fax +40 22 4705062; e-mail martin.huelskamp@uni-koeln.de).
†These authors contributed equally to the work.

SUMMARY

In vascular plants the shoot apical meristem consists of three tissue layers, L1, L2 and the L3, that are kept separate during organ formation and give rise to the epidermis (L1) and the subepidermal tissues (L2, L3). For proper organ development these different tissue layers must interact with each other, though their relative contributions are a matter of debate. Here we use *ANGUSTIFOLIA* (*AN*), which controls cell polarity and leaf shape, to study its morphogenetic function in the epidermis and the subepidermis of *Arabidopsis thaliana*. We show that *ANGUSTIFOLIA* expression in the subepidermis cannot rescue epidermal cell polarity defects, indicating a cell-autonomous molecular function. We demonstrate that leaf width is only rescued by subepidermal *AN* expression, whereas leaf length is also rescued by epidermal expression. Strikingly, subepidermal rescue of leaf width is accompanied by increased cell number in the epidermis, indicating that *AN* can trigger cell divisions in a non-autonomous manner.

Keywords: Arabidopsis, *ANGUSTIFOLIA*, tissue layers, leaf form, chimeras, trichome.

INTRODUCTION

Determinate organs are produced throughout the lifetime of a plant. These organs are formed with a highly predictable size and shape indicating a strict growth control mechanism. However, not much is known about how organ size is regulated with such astonishing precision. Two major parameters of organ growth have been identified: cell number and cell size. Plants with altered parameters often display altered organ size and shape. For example, an increase in cell division rates as seen in plants overexpressing the *AINTEGUMENTA* gene resulted in larger organs (Mizukami and Fischer, 2000). By contrast, in *axr2* mutants a reduction in cell size led to reduced organ size while cell numbers were maintained (Timpte *et al.*, 1992). Cell size is often connected to cellular ploidy level, and an increase in ploidy levels, for instance in tetraploid plants, leads to larger cells and as a consequence to larger organs and plants (Kondorosi *et al.*, 2000).

In addition to the cellular parameters, a supracellular influence of organ growth has also been observed. This is suggested by examples in which the simple positive correlations between cell number or cell size and total organ size are not observed. In some cases a decrease in cellular proliferation is compensated by cell enlargement, suggesting an organ-wide integration system (Tsukaya, 2008). Also changes in shape at the single cell level can be compensated. In the maize mutant *tangled1* cell walls are frequently disorientated and cell shapes are irregular. Nonetheless, the leaves and other organs reach a wild-type size and form (Smith *et al.*, 1996; Cleary and Smith, 1998). In addition several cases have been reported where cell number and cell size could apparently compensate each other, leading to an at least partially restored overall organ size. These cases include compensation for reduced cell numbers by larger cells, and compensation for increased cell volumes by reduction in cell numbers (Tsukaya, 2003). Thus, organ size appears to be regulated not only by cellular parameters but also by supracellular parameters. One possibility for supracellular organization is the application of long-range gradients, as has been postulated by Rolland-Lagen and co-workers (Rolland-Lagan *et al.*, 2003).

One of the most important current questions in the analysis of growth control is how organismal signals are interpreted and executed by cells.

The discussion of the relative contributions of cellular and supracellular effects is still too simplified, as organ form is influenced differently by the tissue layers. Most plant organs consist of three tissue layers (Satina *et al.*, 1940; Satina and Blakeslee, 1941, 1943) that are laid down in the shoot apical meristem: L1, L2 and L3. The three tissue layers are mostly kept separate during ontogenesis because cell divisions in each layer are predominantly anticlinal (perpendicular to the surface) and each meristem layer produces different layers of the organs (Stewart, 1978). In particular, the analysis of plant chimeras with genetically different tissue layers has revealed that all layers are important for development.

In this study we addressed the following question: in which tissues is *ANGUSTIFOLIA* (*AN*) activity necessary to regulate organ shape? The *AN* gene encodes a C-terminal binding protein (CtBPs)/brefeldin A ribosylated substrate (BARS) (Folkers *et al.*, 2002; Kim *et al.*, 2002). Mutations in the *AN* gene result in a pleiotropic phenotype including narrow cotyledons and leaves and twisted siliques, and at the cellular level under-branched trichomes and less-lobed epidermal pavement cells (Koornneef *et al.*, 1982; Hulskamp *et al.*, 1994; Tsukaya *et al.*, 1994; Tsuge *et al.*, 1996). The narrow leaf phenotype is caused by a change in growth directionality of leaf cells and by a decreased number of cells in the width direction.

In this study we genetically created chimeras with wild-type and mutant tissue layers. This was achieved by introducing a wild-type copy of *AN* under the control of tissue layer-specific promoters in *an* mutant plants. We show that expression of *AN* in the epidermis rescues the epidermal cell form defects. Expression in the subepidermis rescues the leaf width phenotype but not the cellular defects in the epidermis, indicating its cell-autonomous action. The effect on overall leaf shape of *AN* is regulated differently by the tissue layers. While the length is rescued by epidermal and subepidermal expression, leaf width is only controlled by the subepidermis. Strikingly, subepidermal rescue is accompanied by a non-cell autonomously regulated increase of epidermal cell number.

RESULTS

Tissue layer specific expression of *ANGUSTIFOLIA*

In order to analyze the role of *AN* in different tissue layers we expressed the *AN* cDNA under two tissue-specific promoters in *an* mutant Arabidopsis plants. The *pAtML1* promoter was used to express *AN* in the epidermis. This promoter was shown to be epidermis-specific during early leaf development, in inflorescences and embryos (Sessions *et al.*, 1999; Savaldi-Goldstein *et al.*, 2007; Takada and Jurgens, 2007). To drive subepidermal expression we used the *phosphoenol-pyruvate-carboxylase* promoter (*pPCAL*) from *Flaveria trinervia* that is known to be active exclusively in subepidermal tissues in *Flaveria*, tobacco (Stockhaus *et al.*, 1994) and Arabidopsis (Bouyer *et al.*, 2008). To ensure that both promoters are suitable for our studies we tested them more carefully. The *pAtML1* promoter was tested with in *pAtML1::NLS-3* × GFP transgenic lines. Epidermis-specific activity of the *AtML1* promoter was found in leaf primordia, old leaves, petals and siliques (Figure 1a–d). The *pPCAL* promoter was tested in *pPCAL::GFP–YFP* and *pPCAL::GUS* transgenic lines. Expression of the *PCAL* promoter was found in cotyledons, rosette leaves, cauline leaves and sepals, but not in roots, hypocotyls, petals and siliques (data not shown). Using *pPCAL::GFP–YFP* and *pPCAL::GUS* lines, the specific expression in subepidermal layers was confirmed in leaf primordia and mature rosette leaves (Figure 1e–i), although the promoter activity in leaf primordia appears to be lower than that in mature rosette leaves. Therefore, both *pAtML1* and *pPCAL* promoters are useful tools for analyzing the role of *AN* in the epidermis and subepidermis for the control of different leaves.

Both constructs, *pAtML1::AN* and *pPCAL::AN*, were expressed in *an* mutant plants to analyze their ability to rescue the leaf phenotype. We used two transgenic lines for each construct for a detailed phenotypic analysis. Real-time PCR revealed that both lines carrying the *pAtML1::AN* construct showed about half the expression level as found in the wild type (Figure 2). The expression levels in the two *pPCAL::AN* lines differed. Line 13 exhibited about 20% of the wild-type level and line 20 about the same level as the wild type (Figure 2), enabling us to evaluate potential dosage dependence for subepidermis-specific *AN* expression.

ANGUSTIFOLIA acts in a cell-autonomous manner

A prerequisite for the analysis of cell layer-specific functions of *AN* is its cell-autonomous function. Its cell-autonomous function in the epidermis was already suggested based on *an* mutant epidermis clones (Hulskamp *et al.*, 1994). Proof of a cell-autonomous function between epidermal and subepidermal layers was provided by our analysis of epidermal pavement cells and trichomes in *an* mutant plants carrying the *pAtML1::AN* and the *pPCAL::AN* constructs. As compared to wild type, trichomes were underbranched in *an* mutants. Trichomes on the first and second leaf of the wild-type ecotype Columbia-0 had 5.7% one-branched, 91% two-branched and 2.7% three-branched trichomes (Figure 3e, Table 1). In *an* mutant plants 18.4% were unbranched and 81.5% were one-branched. Leaves in *an* mutants expressing *AN* in the epidermis showed rescue of the trichome branching phenotype (Figure 3g, Table 1). Expression of *AN* in the subepidermis did not result in a rescue of the trichome branching phenotype (Figure 3h, Table 1).

Epidermal pavement cells normally exhibit a shape like a jigsaw puzzle piece due to the formation of many lobes

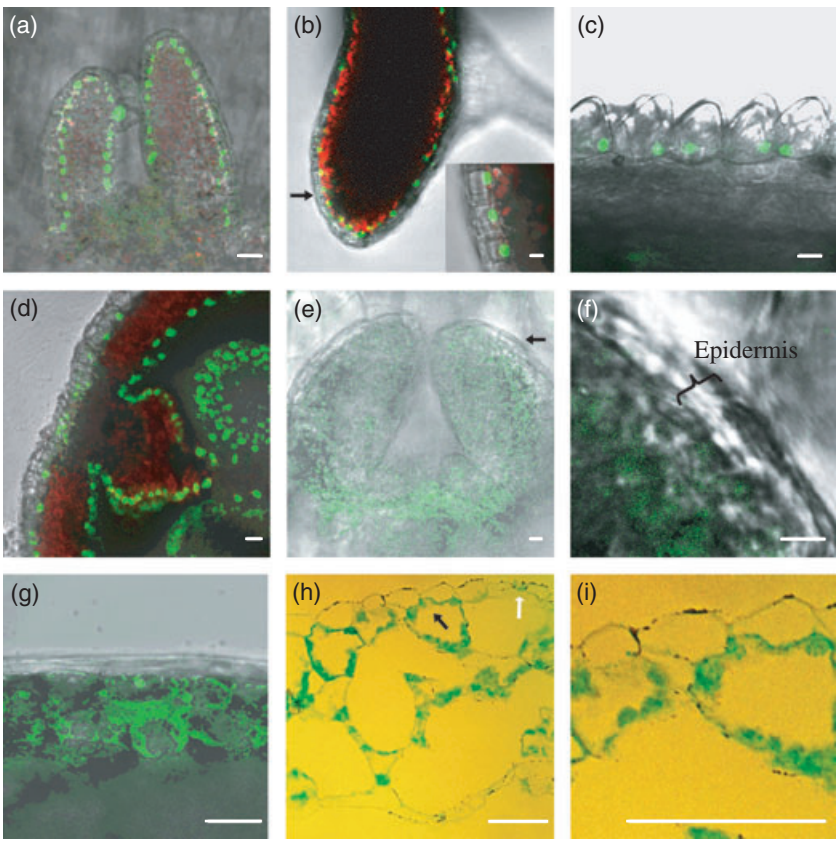

Figure 1. Expression analysis of the *pAtML1* and *pPCAL* promoter in Arabidopsis.
(a–d) *pAtML1* promoter activity as revealed by *pAtML1::NLS-3* × GFP. Note, that the signal is exclusively seen in the epidermis. (a) Leaf primordium. (b) Mature rosette leaf. The inset shows a higher magnification of the region indicated by the arrow. (c) Petal. (d) Silique. Scale bars: 10 μm.
(e–g) Expression of the *pPCAL* promoter as indicated by *pPCAL::GFP:YFP*. The expression is shown in green. Note that the expression is exclusively seen in the subepidermis. (e) Leaf primordium. (f) Higher magnification of the region indicated by the arrow in (e). (g) Mature rosette leaf.
(h) GUS staining of the mature rosette leaves in *pPCAL::GUS* lines. The white arrow points to the stomata.
(i) Higher magnification of the region indicated by the black arrow in (h). Scale bars: 10 μm.

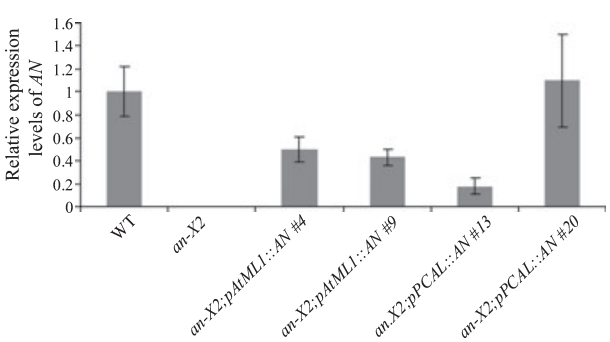

Figure 2. Expression strength in *pPCAL::AN* and *pAtML::AN* lines.
Real-time PCR was used to compare the relative expression levels of *AN* under the *pPCAL* and the *pAtML* promoter with wild type. The *an-X2* allele carries a 5.8 kb inversion leading to a 26 bp deletion of the coding sequence and 3′ untranslated region deletion. Specific primers amplifying the additionally expressed transcripts revealed slightly weaker expression levels of *AN*-RNA expressed in the epidermis and the subepidermis. The mean values of three experiments and the standard deviation are presented.

(Figure 3a). In *an* mutants the formation of lobes was strongly reduced (Figure 3b). In order to quantify the extent of the phenotype we calculated the complexity of cells by determining the relation between the perimeter and the area using the following formula: complexity = $(\text{perimeter})^2/(4\pi \times \text{area})$. If cells are least complex, that is round, the complexity has a value of 1. Irregularities in form and lobes lead to higher complexity values. As shown in Table 2 wild-type pavement cells were most complex with a value of 4.34 ± 1.46 and *an* mutants showed a reduced complexity value of 2.11 ± 0.51. Epidermal expression of *AN* rescued this phenotype (Figure 3c), while plants expressing AN in the subepidermis showed a reduced complexity similar to *an* mutants (Figure 3d, Table 2).

Our data indicate that *AN* or *AN*-dependent downstream processes cannot move from the subepidermal tissue layers to the epidermis.

Subepidermal expression of *AN* but not epidermal expression rescues the leaf width

Both cotyledons and rosette leaves are narrower in *an* mutants than in wild type (Figure 4b,f, Tables 3 and 4). Only expression of *AN* in subepidermal tissues rescued the width defect in *an* mutants (Figure 4d,h, Tables 3 and 4), while *AN* expression in the epidermis had no effect (Figure 4c,g, Tables 3 and 4). These data demonstrated that *AN* was expressed by the *pAtML1* and *pPCAL* promoters as expected and not altered by position effects on the inserted transgene. The *pPCAL::AN* lines are thought not to express relevant *AN* levels in the epidermis because the epidermal phenotypes were not rescued.

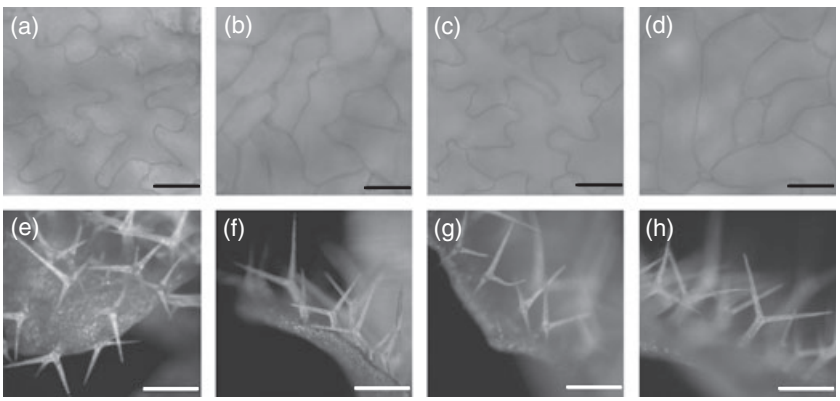

Figure 3. Cell-autonomous behavior of *AN*. Epidermal pavement cells (a–d) and trichomes (e–h) in wild type (a, e) *an-X2* (b, f), *an-X2 pAtML::AN* (c, g) and *an-X2 pPCAL::AN* (d, h). Note that both the epidermal pavement cell phenotype and the trichome phenotype in *an* mutant plants are rescued when *AN* is expressed in the epidermis but not rescued when *AN* is expressed in the subepidermis. Scale bars in (a–d): 50 μm. Scale bars in (e–h): 500 μm.

Table 1 Frequency of trichomes with different branch numbers in wild-type (WT) and transgenic lines on the first two leaves

	Un-branched	One-branched	Two-branched	Three-branched
WT	0.1	5.7 (±4.3)	91.5 (±5.3)	2.7 (±3.9)
an-X2	18.4 (±8)	81.5 (±7.9)	0.1 (±0.7)	0
an-X2 pATML::AN-#4	0.4 (±1)	15.0 (±4.5)	84.0 (±5)	0.8 (±1.7)
an-X2 pATML::AN-#9	0.8 (±1.9)	29.2 (±8.8)	69.6 (±8.8)	0.5 (±1.2)
an-X2 pPCAL::AN-#13	13.6 (±7.9)	85.8 (±7.9)	0.4 (±1.1)	0
an-X2 pPCAL::AN-#20	24.6 (±7.6)	73.6 (±7.2)	1.5 (±1.9)	0.3 (±1)

Table 2 Complexity of epidermal pavement cells

	Complexity[a,b,c]
WT	4.34 (± 1.46)
an-X2	2.11 (±0.51)
an-X2 pAtML1::AN-#4	3.03 (±0.85)
an-X2 pAtML1::AN-#9	2.87 (±0.79)
an-X2 pPCAL::AN-#13	2.12 (±0.56)
an-X2 pPCAL::AN-#20	2.25 (±0.66)

[a]Calculated by complexity = $(\text{perimeter})^2/(4\pi \times \text{area})$.
[b]The values were calculated from 100 cells in each line.
[c]The reduced complexity of epidermal pavement cells in *an* mutants is rescued by expression of *AN* in the epidermis (*pAtML::AN*, *t*-test, $P < 0.001$) but not by expression in the subepidermis (*pPCAL::AN*).

Conversely, the *pAtML1::AN* lines showed no leaf width rescue, indicating the absence of significant *AN* levels in the subepidermis.

Leaf length is rescued by epidermal and subepidermal *AN* expression

Mutant *an* plants exhibit an increased length of cotyledons and rosette leaves. Epidermal as well as subepidermal expression rescued leaf length completely in cotyledons (Table 3). Also *an* mutant rosette leaves were significantly rescued by *AN* expression in both tissue layers, though not completely (Table 4). It is therefore evident that *AN* regulates the length and width of leaves through different tissue layers.

Petal shape is rescued by epidermis-specific expression of *AN*

Mutations in *AN* also result in an altered petal shape. Length but not width is altered when measuring the width at the widest point (Figure 4i,j, Table 5). We also noticed that the general shape was altered, and that in particular the whole basal region was very narrow. Since we did not detect *pPCAL* activity in petals we focused on the lines expressing *AN* in the epidermis. Epidermal expression of *AN* fully rescued petal length, the length/width ratio and overall shape (Figure 4k, Table 5). In order to determine the cellular basis of length changes we determined the number of epidermal cells. These data revealed a strong correlation, suggesting that epidermal *AN* expression regulates organ shape through the cell number (Table 6).

Epidermal cell number is controlled by non-autonomous signaling of subepidermal tissues

The finding that cotyledon and rosette leaf widths are regulated by the subepidermis raises the question of how the epidermis expands accordingly in the absence of *AN* in this layer. We tested the possibility of whether this is due to extra cell divisions. The number of cells along the width axis was reduced in *an* mutants by 21% compared with wild type. Mutant *an* plants expressing *AN* in the epidermis showed no significant difference in the cell number in the width axis. By contrast, subepidermal expression of *AN* resulted in a full rescue of cell number in the epidermis (Table 7). Thus, subepidermal-driven leaf expansion by *AN* is compensated

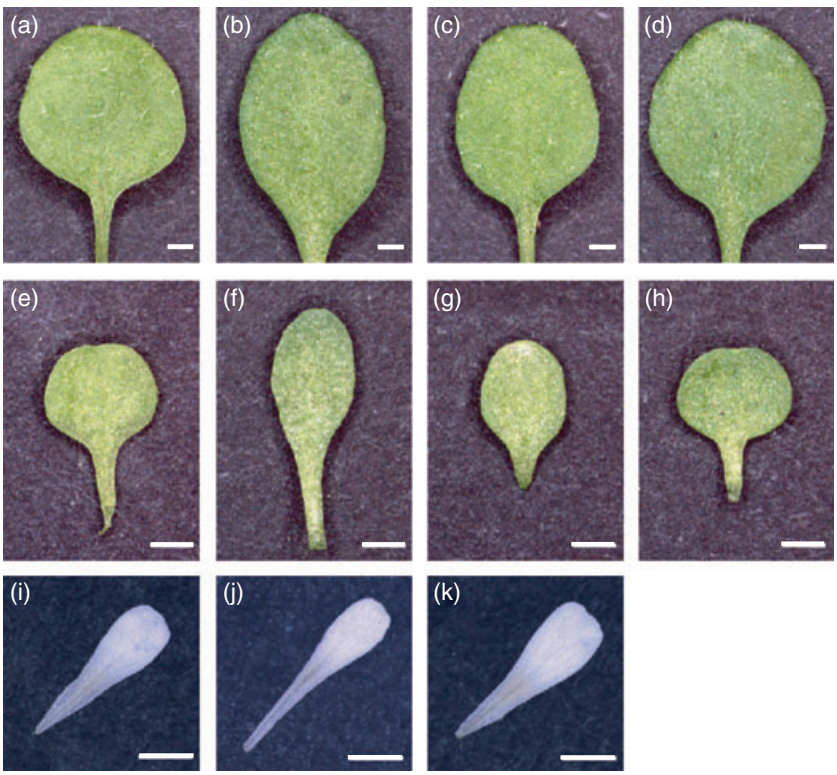

Figure 4. Tissue layer-specific rescue of *AN*.
First pair of rosette leaves (a–d), cotyledons (e–h) and petals (i–k) in wild type (a, e, i) *an-X2* (b, f, j), *an-X2 pAtML::AN* (c, g, k) and *an-X2 pPCAL::AN* (d, h). Subepidermal *AN* expression (d, h) rescues both the length and width phenotype, while epidermal expression of AN rescues the length phenotype (c, g, k). Scale bars: 1 mm.

Table 3 Length and width measurements in cotyledons

	Leaf length (mm)[a]	Leaf width (mm)[a]	Ratio (L/W)[a,b]
WT Col	3.08 (±0.25)	3.07 (±0.23)	1.00 (±0.07)
an-X2	3.94 (±0.39)	2.15 (±0.19)	1.84 (±0.24)
an-X2 pAtML1::AN-#4	2.84 (±0.23)	2.09 (±0.12)	1.36 (±0.10)
an-X2 pAtML1::AN-#9	2.95 (±0.24)	2.24 (±0.17)	1.32 (±0.11)
an-X2 pPCAL::AN-#13	2.64 (±0.33)	2.64 (±0.28)	1.00 (±0.12)
an-X2 pPCAL::AN-#20	2.71 (±0.26)	3.08 (±0.18)	0.88 (±0.07)

WT Col, wild type Columbia-0.
[a]The values are calculated from 50 cotyledons in each line.
[b]The ratios are calculated by the formula: ratio = length (L)/width (W).

Table 4 Length and width measurement in rosette leaves

	Leaf length (mm)[a]	Leaf width (mm)[a]	Ratio (L/W)[a,b]
WT Col	5.98 (±0.25)	5.96 (±0.32)	1.00 (±0.03)
an-X2	7.50 (±0.43)	4.98 (±0.22)	1.51 (±0.09)
an-X2 pAtML1::AN-#4	6.40 (±0.63)	5.08 (±0.32)	1.26 (±0.08)
an-X2 pAtML1::AN-#9	6.61 (±0.53)	4.95 (±0.47)	1.34 (±0.10)
an-X2 pPCAL::AN-#13	7.03 (±0.51)	5.56 (±0.38)	1.27 (±0.08)
an-X2 pPCAL::AN-#20	6.73 (±0.56)	5.78 (±0.39)	1.16 (±0.06)

WT Col, wild type Columbia-0.
[a]The values are calculated from 50 rosette leaves in each line.
[b]The ratios are calculated by the formula: ratio = length (L)/width (W).

Table 5 Length and width measurements in petals

	Petal length (mm)[a,c]	Petal width (mm)[a]	Ratio (L/W) (mm)[a,b,c]
WT	2.77 (±0.20)	0.85 (±0.12)	3.32 (±0.37)
an-X2	3.54 (±0.29)	0.87 (±0.09)	4.18 (±0.58)
an-X2 pAtML1::AN-#4	3.10 (±0.22)	0.95 (±0.08)	3.24 (±0.36)
an-X2 pAtML1::AN-#9	2.88 (±0.12)	0.84 (±0.06)	3.59 (±0.29)

WT, wild type.
[a]The values are calculated from 30 petals in each line.
[b]The ratios are calculated by the formula: ratio = length (L)/width (W).
[c]The length and the length/width ratio is significantly rescued in *an-X2 pAtML1::AN* plants (*pAtML1::AN*, *t*-test, $P < 0.001$).

Table 6 Cell numbers along the length and width axis of petals in wild type (WT), *an-X2*, *an-X2 pAtML1::AN* lines

	Cells in length[a,c]	Cells in width[a]	Ratio (L/W)[a,b,c]
WT	100.3 (±7.97)	70.0 (±4.6)	1.44 (±0.11)
an-X2	129.0 (±12.53)	70.0 (±3.9)	1.84 (±0.18)
an-X2 pAtML1::AN-#4	107.5 (±6.22)	74.9 (±5.1)	1.44 (±0.15)
an-X2 pAtML1::AN-#9	102.0 (±5.51)	70.2 (±3.5)	1.46 (±0.14)

[a]The values were calculated from 10 petals in each line.
[b]The ratios are calculated by the formula: ratio = cell number in length (L)/cell number in width (W).
[c]The cell number along the length and the cell number length/width ratio is significantly rescued in *an-X2 pAtML1::AN* plants (*pAtML1::AN*, *t*-test, $P < 0.001$).

Table 7 Cell numbers along the rosette leaf width and length axis of wild type (WT), *an-X2*, *an-X2 pAtML1::AN* lines and *an-X2 pPCAL::AN* lines

	Cell number along length axis[a,c]	Cell number along width axis[a]	Ratio (L/W)[a,b,c]
WT Col	70.7 (±2.5)	85.7 (±4.8)	0.83 (±0.06)
an-X2	85.9 (±3.9)	68.0 (±2.8)	1.26 (±0.06)
an-X2 pAtML1::AN-#4	77.5 (±3.7)	67.0 (±7.5)	1.17 (±0.18)
an-X2 pAtML1::AN-#9	81.3 (±4.2)	72.1 (±4.2)	1.13 (±0.08)
an-X2 pPCAL::AN-#13	84.4 (±4.5)	84.6 (±6.0)	1.00 (±0.09)
an-X2 pPCAL::AN-#20	82.5 (±4.1)	86.2 (±4.4)	0.96 (±0.08)

[a]The values are calculated from 10 rosette leaves in each line.
[b]The ratios are calculated by the formula: ratio = cell number in length (L)/cell number in width (W).
[c]The cell number along the length (*pAtML1::AN*, *t*-test, $P < 0.001$) and the cell number along the width (*pPCAL::AN*, *t*-test, $P < 0.001$) is rescued significantly in *pAtML1::AN* and *pPCAL::AN* plants, respectively.

in the *an* mutant epidermis by extra cell divisions. This finding indicates that *AN* can regulate cell divisions in a non-autonomous manner.

Epidermal *AN* expression is sufficient to rescue the an silique phenotype

One striking phenotype of *an* mutants is the twisting of siliques. Although a comparative analysis was precluded because the *pPCAL* promoter is not active in siliques we wanted to know whether epidermal expression can rescue this phenotype. Siliques in plants rescued by epidermal *AN* expression were indistinguishable from the wild type (Figure 5, Table 8). While the fraction of twisted siliques is about 68% in *an* mutants, *an-X2 pAtML::AN* plants have about 14% twisted siliques. Also the angle of twisting goes down from 110° degree to 13–14° in the rescued plants.

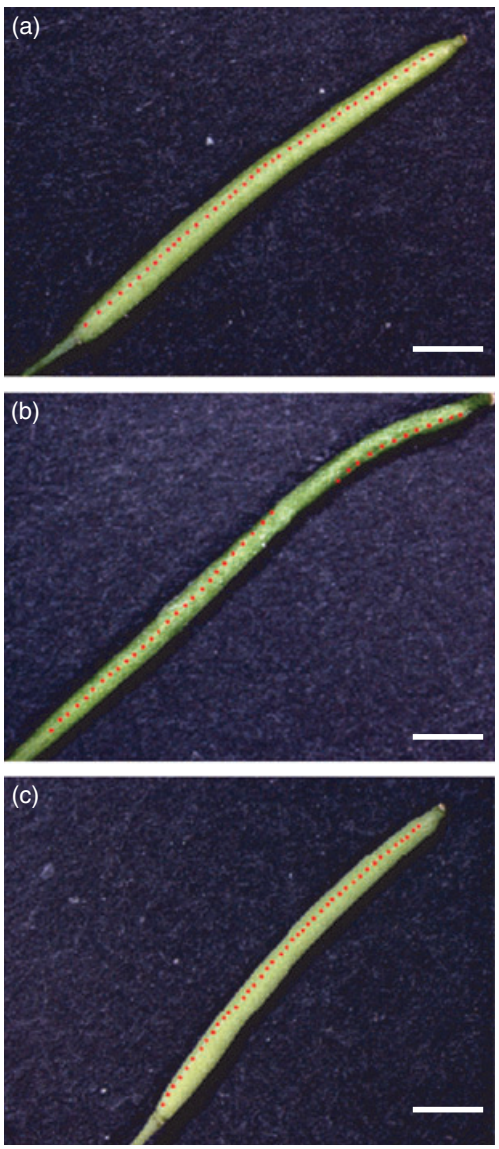

Figure 5. Silique twisting in wild type (WT), *an-X2* and *an-X2 pAtML1::AN* lines.
Siliques in WT (a), *an-X2* (b), *an-X2 pAtML::AN* (c). The valve attachment site is highlighted by a dashed line to indicate the twisting of the silique. Scale bars: 2 mm.

DISCUSSION

Which layer is the form-giving tissue in Arabidopsis?

Clonal analysis has been used to create a fate map for the root and the shoot in Arabidopsis (Furner and Pumfrey, 1992; Irish and Sussex, 1992; Dolan *et al.*, 1993, 1994; Schnittger *et al.*, 1996; Saulsberry *et al.*, 2002). The fate mapping data obtained for the three meristematic cell layers in the shoot apical meristem showed that predictions can only be made in a general and probabilistic way, indicating that cell fate determination occurs largely independently of cell lineage and in a position-dependent fashion. A few examples indicate that the L2 layer is important for organ shape (Stewart, 1978; Tilney-Bassett, 1986; Szymkowiak and Susse, 1996). Periclinal chimeras between *Solanum luteum* (simple leaves) *and Solanum lycopersicum* (compound leaves) revealed that the form of the leaf depends on the genotype of the L2 layer (Jorgensen and Crane, 1928). The L1 and L3 layer did not contribute to the overall leaf form. Each layer, however, controlled cell differentiation, autonomously. A role of the L2 and the L3 layers was reported for normal development of stamen and carpel during flower development (Sieburth *et al.*, 1998; Vincent *et al.*, 2003) and the L3 layer was shown to control floral meristem size and carpel number (Szymkowiak and Sussex, 1992). But the L1 layer is also important for organ shape and general plant growth. For example, petal shape is controlled by the L1 layer (Vincent *et al.*, 2003). Recently, it was demonstrated that the epidermis is important for brassinoid-dependent plant growth (Savaldi-Goldstein

Table 8 Twisting of siliques in wild type (WT), *an-X2* and *an-X2 pAtML1::AN* lines

	Twisting angle[a,b]	Percentage of twisted silique[a,b]
WT	3.6 (±17.8)	0.04
an-X2	109.8 (±123.7)	0.64
an-X2 pAtML1::AN-#4	12.6 (±31.5)	0.14
an-X2 pAtML1::AN-#9	14.4 (±18.0)	0.14

[a]The values are calculated from 50 siliques in each line.
[b]The twisted silique phenotype of *an* mutants was significantly rescued by expression of *AN* in the epidermis (*pAtML1::AN*, *t*-test, $P < 0.001$).

et al., 2007). The picture emerging from these data is that the relative importance of tissue layers may vary between different organs and developmental stages. These general notions derived from various experiments are confirmed by us at the level of one single morphogenesis gene. Our findings indicate that *AN* regulates organ shape through the epidermis and subepidermis, though their role differs for length and width regulation.

How does the epidermis respond to subepidermal growth?

Several lines of evidence indicate that organ growth is controlled at the supracellular level and that growth changes cannot be attributed to one growth parameter alone (Fleming, 2002; Reinhardt and Kuhlemeier, 2002; Tsukaya, 2002). Mutations in the *TANGLED* gene of maize cause irregular division patterns without affecting the leaf size or shape, indicating that defects in the orientation of cell divisions can be compensated at the organ level (Smith *et al.*, 1996). Compensatory effects were in particular observed for cell divisions versus changes in cell volume (Fleming, 2002; Reinhardt and Kuhlemeier, 2002; Tsukaya, 2002). For example, slowing down cell division rates in tobacco did not affect the leaf shape or size because of an increased cell volume (Hemerly *et al.*, 1995). Conversely, acceleration of cell divisions in tobacco affected the rate of organ initiation but not the leaf size (Cockcroft *et al.*, 2000). These observations indicate that cell divisions and cell growth are to some extent interchangeable processes during plant growth. Our observation that leaf width of *an*-chimera leaves in Arabidopsis is controlled by the subepidermis demonstrates that the subepidermal cells can control the growth of the epidermis. We show that the epidermal cell number in the width direction is completely restored in plants expressing *AN* in the subepidermis, indicating that extra cell divisions are triggered in a non-cell autonomous manner.

The finding that the epidermis compensates extra growth of the underlying tissues raises the question of how this is achieved. The simplest explanation is that physical forces generated by subepidermal growth trigger growth in the epidermis. The existence of such a mechanism is suggested by the finding that the application of expansins on shoot apical meristems could trigger local outgrowth (Fleming *et al.*, 1997). As the only known function of expansins is cell wall loosening it is conceivable that the initiation of growth was triggered by changes in the biophysical equilibrium. However, *low cell density* (*lcd*) mutants, which show reduced cell number in the subepidermis, exhibit no obvious changes in leaf shape (Barth and Conklin, 2003), suggesting that biophysical forces may not be important during the development of leaf shape. The second possibility is that specific *AN*-dependent signals from the subepidermis promote cell divisions in the epidermis. In one case known cell cycle regulators were shown to act in a non-cell autonomous manner. The cyclin-dependent kinase inhibitor ICK1/KRP1 can move between cells and has been suggested to link cell cycle control in single cells with the supracellular organization of tissues (Weinl *et al.*, 2005).

What do we learn about *AN* function?

All aspects of the *an* phenotype indicate that *AN* is involved in the establishment of polarity. At the cellular level, epidermal pavement cells show alterations in polarity, and in trichomes the normally asymmetric trichomes are symmetric. At the organ level *AN* controls the width of leaves via two growth parameters: polarity of cells and cell divisions. The reduction of cell divisions along the leaf width axis could in principle be due to *AN*-specific cell division defects. This seems not to be true, as *an*-mutant epidermis can compensate subepidermal lateral growth by extra cell divisions along the width direction. This is an important conclusion because this indicates that *AN* is not necessary for cell divisions but rather controls cell divisions in a non-autonomous manner.

EXPERIMENTAL PROCEDURES

Expression constructs

For expression in the mesophyll and parenchyma tissue, a 2.2 kb *Hin*dIII/*Sma*I fragment from the 5′ upstream region of the *PPCA1* gene from *Flaveria trinervia* was utilized (Stockhaus *et al.*, 1994). To achieve expression within the epidermis a 3.5 kb fragment upstream of the beginning of exon 1 of the *ML1* gene from Arabidopsis was used (Sessions *et al.*, 1999).

To generate the *pPCAL::GFP5* construct (pART1), the *pPCAL* promoter was excised from ppcA-L-Ft pBS (a gift from Peter Westhoff) with *Hin*DIII and *Sma*I and inserted into the *Hin*DIII and *Xba*I site, treated with Klenow fragment, of *pBIN19mGFP5* (a gift from Jim Haseloff). To generate the *pPCAL::AN* construct (pART2), the *AN* cDNA was excised from pBSAN (Folkers *et al.*, 2002) with *Eco*RV, and *Sac*I and inserted into pART1 digested with *Bam*HI, treated with Klenow fragment, and *Sac*I. For further usage, a *pPCAL* expression vector with a small multiple cloning site was generated by excising the *AN* gene from pART2 with *Bam*HI and subsequent religation to yield plasmid pART4. Next, an *ML1* expression vector with a small multiple cloning site was generate by digesting pART4 with *Hin*DIII, treated with Klenow fragment, and *Cfr*9I (to excise the *pPCAL* promoter), and inserting the *ML1* promoter from pAS99 (a kind gift of Allen Sessions) digested with *Xho*I, treated with

Klenow fragment, and *Cfr*9I to yield plasmid pART5. To generate the *pML1::AN* construct (pART6), the *AN* cDNA was excised with *Bam*HI from pBSAN and inserted into *Bam*HI-digested pART5. To generate the *pPCAL::GUS* construct (pART22) the *pPCAL* promoter was excised from ppcA-L-Ft pBS with *Hin*DIII and *Sma*I and inserted into *Hin*DIII/*Sma*I-digested pBI 101 (Jefferson, 1987). Unless stated otherwise, all manipulations were performed using standard molecular methods.

Plant transformation and culturing

Plants were grown under long-day conditions at 25°C. The wild-type strain used in this work was Columbia-0. The *an-X2* allele carries a 5.8 kb inversion leading to a 26 bp deletion of the coding sequence and of the 3′ untranslated region (UTR) (Folkers *et al.*, 2002). *Agrobacterium tumefaciens* GV3101 pMP90 mediated transformation of Arabidopsis plants was performed as described by Clough and Bent (Clough and Bent, 1998).

Real-time PCR analysis

The expression of *AN* was analyzed by real-time quantitative RT-PCR using SYBR-Green in the GeneAmp 5700 sequence Detection System (Applied Biosystems, http://www.appliedbiosystems.com). The Arabidopsis *ACTIN2* gene was used as standard (actin2 for: ATGGAAGCTGCTGGAATCCAC; actin2 rev: TTGCTCATACGG TCAGCGATG). The deleted 26 bp region in *an-X2* was used for primer design to distinguish the functional full *AN* mRNA and the endogenous deleted mRNA in *an-X2* (pair2 for: CTCTGGAC-GAATGTCGGCTTG; pair2 rev: TTAATCGATCCAACGTGTGATAC). The calculated relative expression values were normalized to the wild type (WT) expression level, WT = 1.

The measurement of complexity, cell number length and width

For all measurements the first and second leaves of 4-week-old plants were taken. To determine the complexity, leaves were incubated in 70% (v/v) ethanol and analysed with a Leica DM RA2 microscope (Leica, http://www.leica-microsystems.com/). The DISKUS software package, version 4.30.19 (Carl H. Hilgers-Technisches Büro, http://www.hilgers.com/) was used to surround a single cell and calculate the perimeter and the area of a cell. The width was determined at the widest region of cotyledons, rosette leaves and petals.

Histology

The GUS stained plant material was analyzed either under the binocular or microscope. To determine if the *pPCAL* promoter is layer specific, GUS stained and fixated leaves were embedded in plastic after Spurr (1969). ERL-4206 was replaced by the cycloaliphatic epoxy resin ERL-4221 D and was used in the same concentrations as described by Spurr. After embedding, sections of around 250 μm were made and analyzed under the microscope.

ACKNOWLEDGEMENTS

We would like to thank G. Jürgens for providing the *pAtML1::NLS-3* × GFP line and P. Westhoff for the *pPCAL* promoter. We would like to thank the lab members for critically reading the manuscript. This work was supported by the DFG SPP 1111 to MH. YB is supported by the International Max-Planck-Research School, IMPRS.

REFERENCES

Barth, C. and Conklin, P.L. (2003) The lower cell density of leaf parenchyma in the Arabidopsis thaliana mutant lcd1-1 is associated with increased sensitivity to ozone and virulent Pseudomonas syringae. *Plant J.* **35**, 206–218.

Bouyer, D., Geier, F., Kragler, F., Schnittger, A., Pesch, M., Wester, K., Balkunde, R., Timmer, J., Fleck, C. and Hulskamp, M. (2008) Two-dimensional patterning by a trapping/depletion mechanism: the role of TTG1 and GL3 in Arabidopsis trichome formation. *PLoS Biol.* **6**, e141.

Cleary, A.L. and Smith, L.G. (1998) The Tangled1 gene is required for spatial control of cytoskeletal arrays associated with cell division during maize leaf development. *Plant Cell*, **10**, 1875–1888.

Clough, S. and Bent, A. (1998) Floral dip: a simplified method for Agrobacterium-mediated transformation of Arabidopsis thaliana. *Plant J.* **16**, 735–743.

Cockcroft, C.E., den Boer, B.G., Healy, J.M. and Murray, J.A. (2000) Cyclin D control of growth rate in plants. *Nature*, **405**, 575–579.

Dolan, L., Janmaat, K., Willemsen, V., Linstead, P., Poethig, S., Roberts, K. and Scheres, B. (1993) Cellular organisation of the *Arabidopsis thaliana* root. *Development*, **119**, 71–84.

Dolan, L., Duckett, C.M., Grierson, C., Linstead, P., Schneider, K., Lawson, E., Dean, C., Poethig, S. and Roberts, K. (1994) Clonal relationships and cell patterning in the root epidermis of *Arabidopsis*. *Development*, **120**, 2465–2474.

Fleming, A.J. (2002) The mechanism of leaf morphogenesis. *Planta*, **216**, 17–22.

Fleming, A.J., McQueen-Mason, S., Mandel, T. and Kuhlemeier, C. (1997) Induction of leaf primordia by the cell wall protein expansin. *Science*, **276**, 1415–1418.

Folkers, U., Kirik, V., Schobinger, U. *et al.* (2002) The cell morphogenesis gene ANGUSTIFOLIA encodes a CtBP/BARS-like protein and is involved in the control of the microtubule cytoskeleton. *EMBO J.* **21**, 1280–1288.

Furner, I.J. and Pumfrey, J.E. (1992) Cell fate in the shoot apical meristem of *Arabidopsis thaliana*. *Development*, **115**, 755–764.

Hemerly, A., Engler, J.A., Bergounioux, C., Montagu, M.v., Engler, G., Inze, D. and Ferreira, P. (1995) Dominant negative mutants of the Cdc2 kinase uncouple cell division from iterative plant development. *EMBO J.* **14**, 3925–3936.

Hulskamp, M., Misera, S. and Jürgens, G. (1994) Genetic dissection of trichome cell development in *Arabidopsis*. *Cell*, **76**, 555–566.

Irish, V.F. and Sussex, I.M. (1992) A fate map of the *Arabidopsis* embryonic shoot apical meristem. *Development*, **115**, 745–753.

Jefferson, R.A. (1987) Assaying chimeric genes in plants: the GUS gene fusion system. *Plant Mol. Biol. Rep.* **5**, 387–405.

Jorgensen, C.A. and Crane, M.B. (1928) Formation and Morphology of Solanum Chimaeras. *J. Genet.* **18**, 247–273.

Kim, G.T., Shoda, K., Tsuge, T., Cho, K.-H., Uchimiya, H., Yokoyama, R., Nishitani, K. and Tsukaya, H. (2002) The ANGUSTIFOLIA gene of Arabidopsis, a plant CtBP gene, regulates leaf-cell expansion, the arrangement of cortical microtubules in leaf cells and expression of a gene involved in cell-wall formation. *EMBO J.* **21**, 1267–1279.

Kondorosi, E., Roudier, F. and Gendreau, E. (2000) Plant cell-size control: growing by ploidy? *Curr. Opin. Plant Biol.* **3**, 488–492.

Koornneef, M., Dellaert, L.W.M. and Veen, J.H.v.d. (1982) EMS-and radiation-induced mutation frequencies at individual loci in *Arabidopsis thaliana* (L.) Heynh. *Mutat. Res.* **93**, 109–123.

Mizukami, Y. and Fischer, R.L. (2000) Plant organ size control: AINTEGUMENTA regulates growth and cell numbers during organogenesis. *Proc. Natl Acad. Sci. USA*, **97**, 942–947.

Reinhardt, D. and Kuhlemeier, C. (2002) Plant architecture. *EMBO Rep.* **3**, 846–851.

Rolland-Lagan, A.G., Bangham, J.A. and Coen, E. (2003) Growth dynamics underlying petal shape and asymmetry. *Nature*, **422**, 161–163.

Satina, S. and Blakeslee, A.F. (1941) Periclinal chimeras in *Datura stramonium* in relation to development of leaf and flower. *Am. J. Bot.* **28**, 862–871.

Satina, S. and Blakeslee, A.F. (1943) Periclinal chimeras in *Datura* in relation to the development of the carpel. *Am. J. Bot.* **30**, 453–462.

Satina, S., Blakeslee, A.F. and Avery, A.G. (1940) Demonstration of the three germ layers in the shoot apex of Datura by means of induced polyploidy in periclinal chimeras. *Am. J. Bot.* **27**, 895–905.

Saulsberry, A., Martin, P.R., O'Brien, T., Sieburth, L.E. and Pickett, F.B. (2002) The induced sector Arabidopsis apical embryonic fate map. *Development*, **129**, 3403–3410.

Savaldi-Goldstein, S., Peto, C. and Chory, J. (2007) The epidermis both drives and restricts plant shoot growth. *Nature*, **446**, 199–202.

Schnittger, A., Grini, P.E., Folkers, U. and Hulskamp, M. (1996) Epidermal fate map of the Arabidopsis shoot meristem. *Dev. Biol.* **175**, 248–255.

Sessions, A., Weigel, D. and Yanofsky, M. (1999) The Arabidopsis thaliana MERISTEM LAYER1 promoter specifies epidermal expression in meristems and young primordia. *Plant J.* **20**, 259–263.

Sieburth, L.E., Drews, G.N. and Meyerowitz, E.M. (1998) Non-autonomy of *AGAMOUS* function in flower development:use of a Cre/loxP method for mosaic analysis in *Arabidopsis*. *Development*, **125**, 4303–4312.

Smith, L.G., Hake, S. and Sylvester, A.W. (1996) The tangled-1 mutation alters cell division orientations throughout maize leaf development without altering leaf shape. *Development*, **122**, 481–489.

Spurr, A.P. (1969) A low-viscosity epoxy resin embedding medium for electron microscopy. *J. Ultrastruct. Res.* **26**, 31–43.

Stewart, R.N. (1978) Ontogeny of the primary body in chimeral forms of higher plants. In *The Clonal Basis of Development* (Subtelny, S. and Sussex, I.M., eds). New York, San Francisco, London: Academic Press, pp. 131–160.

Stockhaus, J., Poetsch, W., Steinmuller, K. and Westhoff, P. (1994) Evolution of the C4 phosphoenolpyruvate carboxylase promoter of the C4 dicot Flaveria trinervia: an expression analysis in the C3 plant tobacco. *Mol. Gen. Genet.* **245**, 286–293.

Szymkowiak, E.J. and Susse, I.M. (1996) What chimeras can tell us about plant development. *Annu. Rev. Plant Physiol. Plant Mol. Biol.* **47**, 351–376.

Szymkowiak, E.J. and Sussex, I.M. (1992) The internal meristem layer (L3) determines floral meristem size and carpel number in tomato periclinal chimeras. *Plant Cell*, **4**, 1089–1100.

Takada, S. and Jurgens, G. (2007) Transcriptional regulation of epidermal cell fate in the Arabidopsis embryo. *Development*, **134**, 1141–1150.

Tilney-Bassett, R.A.E. (1986) *Plant Chimeras*. London: Edward Arnold Publishers Ltd.

Timpte, C.S., Wilson, A.K. and Estelle, M. (1992) Effects of the *axr2* mutation of *Arabidopsis* on cell shape in hypocotyl and inflorescence. *Planta*, **188**, 271–278.

Tsuge, T., Tsukaya, H. and Uchimiya, H. (1996) Two independent and polarized processes of cell elongation regulate leaf blade expansion in Arabidopsis thaliana (L.) Heynh. *Development*, **122**, 1589–1600.

Tsukaya, H. (2002) Interpretation of mutants in leaf morphology: genetic evidence for a compensatory system in leaf morphogenesis that provides a new link between cell and organismal theories. *Int. Rev. Cytol.* **217**, 1–39.

Tsukaya, H. (2003) Organ shape and size: a lesson from studies of leaf morphogenesis. *Curr. Opin. Plant Biol.* **6**, 57–62.

Tsukaya, H. (2008) Controlling size in multicellular organs: focus on the leaf. *PLoS Biol.* **6**, 1373–1376.

Tsukaya, H., Tsuge, T. and Uchimiya, H. (1994) The cotyledon: a superior system for studies of leaf development. *Planta*, **195**, 309–312.

Vincent, C.A., Carpenter, R. and Coen, E.S. (2003) Interactions between gene activity and cell layers during floral development. *Plant J.* **33**, 765–774.

Weinl, C., Marquardt, S., Kuijt, S.J., Nowack, M.K., Jakoby, M.J., Hulskamp, M. and Schnittger, A. (2005) Novel Functions of Plant Cyclin-Dependent Kinase Inhibitors, ICK1/KRP1, Can Act Non-Cell-Autonomously and Inhibit Entry into Mitosis. *Plant Cell*, **17**, 1704–1722.

